Strongly coupled quantum Otto cycle with single qubit bath

Sagnik Chakraborty ,[*] Arpan Das ,[†] and Dariusz Chruściński [‡]
Institute of Physics, Faculty of Physics, Astronomy and Informatics, Nicolaus Copernicus University,
Grudziądzka 5/7, 87-100 Toruń, Poland

(Received 12 July 2022; revised 10 October 2022; accepted 15 November 2022; published 26 December 2022)

We discuss a model of a closed quantum evolution of two qubits where the joint Hamiltonian is so chosen such that one of the qubits acts as a bath and thermalizes the other qubit which is acting as the system. The corresponding exact master equation for the system is derived. Interestingly, for a specific choice of parameters the master equation takes the Gorini-Kossakowski-Lindblad-Sudarshan (GKLS) form, with constant coefficients representing pumping and damping of a single qubit system. Based on this model we construct an Otto cycle connected to a single qubit bath and study its thermodynamic properties. Our analysis goes beyond the conventional weak coupling scenario and illustrates the effects of finite baths, including non-Markovianity. We find closed form expressions for efficiency (coefficient of performance), power (cooling power) for the heat engine regime (refrigerator regime), and for different modifications of the joint Hamiltonian.

DOI: 10.1103/PhysRevE.106.064133

I. INTRODUCTION

In the last few decades new experimental techniques [1–5] have been developed which enabled the study of particles and phenomena at a length scale where quantum effects play a dominant role. In these studies the quantum systems interact with their ambient environment with varying degrees of isolation. Mostly systems exhibit significant variation in their behavior as a result of weak or strong interaction with the environment. This has resulted in a renewed focus on the study of quantum systems which are open to the environment [6]. When the interaction between the system and the environment is weak, one can microscopically derive its evolution [6,7] through a series of approximations (Born-Markov and secular) in the form of the celebrated Gorini-Kossakowski-Lindblad-Sudarshan (GKLS) master equation [8,9],

$$\frac{d\rho}{dt} = -i[H_S, \rho] + \sum_{k=1}^{n} \gamma_k \left(A_k \rho A_k^\dagger - \frac{1}{2}\{A_k^\dagger A_k, \rho\} \right), \qquad (1)$$

where A_k's are the jump operators, H_S is the (effective) system Hamiltonian, and the rates $\gamma_k \geqslant 0$ for all k. The corresponding evolution is governed by the Markovian semigroup $\Lambda_t = e^{t\mathcal{L}}$. However, for a vast majority of dynamics, interaction is not weak and all the approximations used to derive master equations in GKLS form are not valid. Consequently, such general closed form master equations do not exist when the interaction is not weak. In this case one often uses the corresponding master equation with time-dependent generator, i.e., all objects appearing in (1) are in general time dependent. Interestingly, when time-dependent rates satisfy $\gamma_k(t) \geqslant 0$, we call the corresponding evolutions completely positive divisible or CP divisible [10–15]. This means that the corresponding dynamical map Λ_t satisfies the following composition law:

$$\Lambda_t = V_{t,s}\Lambda_s, \qquad (2)$$

and the corresponding propagator $V_{t,s}$ is completely positive and trace preserving (CPTP) for all $t \geqslant s$. CP-divisible evolutions are usually called Markovian. Also, in this paper we will consider CP divisibility as the criterion for Markovianity. Note that semigroup master equations are also Markovian according to this criterion. Interestingly, there are alternate formulations of Markovianity, namely, the information flow approaches, where a backflow of information from the environment to the system gives rise to non-Markovianity [15–18], but for all these approaches CP divisibility serves as a sufficient criterion. Another approach to quantum (non)Markovian dynamics uses the structure of multitime correlations, which are built during the evolution of the system and environment [12,19–22]. This concept of quantum Markovianity is closely related to the well-known quantum regression theorem [12,23–25].

Theory of open quantum systems provides a solid foundation to the emergent field of quantum thermodynamics [26–28]. The dynamical framework of quantum mechanics allows one to address finite time thermodynamics processes. Specifically, in the weak coupling limit, the microscopically derived Markovian master equation (also known as Davies construction [7]) in the GKLS form gives a consistent and universal description of the basic thermodynamic laws [26,29,30]. Originally, Davies construction was engineered for the time-independent system Hamiltonian. Later on it was generalized for the time-dependent scenarios [31–35]. Beyond the weak coupling approximation, where non-Markovianity inevitably enters into the picture, it is not straightforward to establish a consistent framework of thermodynamics, largely due to the unavailability of a unique closed form master equation as mentioned before.

---

[*] sagnik@umk.pl
[†] arpand@umk.pl
[‡] darch@fizyka.umk.pl

Consequently, a number of approaches [36–46] have been proposed to deal with strong interaction without compromising the thermodynamic consistency. One of the major applications of quantum thermodynamics is the study of quantum thermal machines [30,31,47,48], which are typically restricted to the weak coupling scenario. New experimental techniques [49–55] to access the strongly coupled regime and recent theoretical progresses have now opened an avenue to consider the performance of thermal machines beyond the weak coupling scenario [56–65]. In general, it has been observed that the strong coupling effect reduces the performance of a thermal machine [57,62,63,66,67]. On the other hand, there are several studies [68–71] that showed the non-Markovian effect is actually beneficial for enhancing performance, even in the regime of weak coupling [57,68]. Although there are some objections [72–74] to this non-Markovian boosting due to the neglecting of the coupling and decoupling cost, recently a genuine non-Markovian advantage has been reported [75], taking into account these previous shortcomings. Evidently, it is an intriguing task to investigate the interplay between strong interaction and non-Markovianity [76] with respect to thermodynamic tasks, and it still remains a largely unexplored area.

With this goal, here we consider a model of quantum Otto cycle, where the working medium qubit is connected to another single qubit (working as bath) with arbitrary interaction strength. Notably, in Refs. [77,78] the Otto cycle was implemented on a quantum harmonic oscillator where another harmonic oscillator acted as the bath. In our model, following Ref. [79], we devise a two-qubit unitary evolution such that the exact reduced dynamics of the working medium resembles a semigroup master equation, i.e., in the GKLS form with constant coefficients, representing pumping and damping of a single qubit system. There are several advantages for choosing this model. First, we go beyond the weak coupling approximation and yet get the exact dynamics in GKLS form. Second, by tweaking the interaction Hamiltonian, we can make the dynamics non-Markovian. This gives us a way to study strong coupling and non-Markovianity at the same time. Finally, we have control over the thermalization process taking place in contact with a finite bath. We work out analytical expressions for efficiency (coefficient of performance) and power (cooling power) for the Otto engine (refrigerator), employing the thermodynamic framework suited for strong coupling. We notice that the transition from a Markovian to non-Markovian scenario gives a better performance, even in the regime of strong interaction.

This paper is organized as follows. In Sec. II we give a short introduction to the Otto cycle with a conventional weak coupling approximation. In Sec. III A we discuss the strong coupling formalism we use in our paper. Next we describe our model of qubit bath in Sec. III B. Implementation of the Otto cycle is described in Sec. III C. In Sec. III D we discuss the thermodynamic implications of Markovian and non-Markovian dynamics. Finally, in Sec. IV we conclude.

II. WEAKLY COUPLED OTTO CYCLE

We present a brief discussion of the conventional Otto cycle where the working medium (WM) with Hamiltonian $H_{\rm S}$ is weakly connected to two thermal baths, one at a time, with temperatures T_h and T_c ($T_h > T_c$), respectively. The setup is described by the total Hamiltonian,

$$H(t) = H_{\rm S}(t) + H_{B_h} + H_{B_c} + H_{\rm SB}(t), \tag{3}$$

where $H_{\rm B_h}$, $H_{\rm B_c}$ are the self-Hamiltonians of the hot and cold bath, respectively, and $H_{\rm SB}(t) = H_{\rm SB}^h(t) + H_{\rm SB}^c(t)$ denotes the interaction Hamiltonian. The cycle consists of four strokes as described below. A schematic diagram of the cycle is given in Fig. 1(a). For simplicity we take $\hbar = k_{\rm B} = 1$. We here consider that the time dependence of the WM Hamiltonian is controlled through an external parameter $\omega(t)$, and we write the system Hamiltonian as $H_{\rm S}(\omega(t))$. We also denote $H_{S,\alpha}$ as the WM Hamiltonian at each point of the schematic of Fig. 1(a), with $\alpha = \{A, B, C, D\}$.

First stroke. Initially [point A in the schematic diagram 1(a)], the WM is prepared in the state ρ_S^A with Hamiltonian $H_{S,A} = H_{\rm S}(\omega = \omega_A) \equiv H_{\rm S}(\omega_A)$, in equilibrium with the cold bath. Baths are assumed to be always in equilibrium state with their respective Hamiltonians and temperatures. Therefore the initial joint state of the system-bath setup can be written as

$$\rho_{\rm tot}^A = \rho_S^A \otimes \rho_B^c = \frac{e^{-\beta_c H_{\rm S}(\omega_A)}}{{\rm Tr}[e^{-\beta_c H_{\rm S}^A}]} \otimes \frac{e^{-\beta_c H_{\rm Bc}}}{{\rm Tr}[e^{-\beta_c H_{\rm Bc}}]}. \tag{4}$$

The first stroke is unitary, where the WM is decoupled from the bath and the WM Hamiltonian $H_{\rm S}(\omega(t))$ is changed from $H_{S,A} = H_{\rm S}(\omega_A)$ at point A to $H_{S,B} = H_{\rm S}(\omega_B)$ at point B in a time duration τ_{u1}. The final state of the WM after the first unitary stroke is

$$\rho_S^B = U_1 \rho_S^A U_1^\dagger, \tag{5}$$

where $U_1 = \mathcal{T} \exp[-i\int_{t_A}^{t_B} H_{\rm S}(\omega(t))dt]$ is the unitary operator, and $\mathcal{T}$ represents time ordering.

Second stroke. In this stroke from point B to C, the WM is connected to the hot bath at inverse temperature β_h for a time interval τ_h, while keeping the WM Hamiltonian fixed at $H_{\rm S}(\omega_B)$ throughout the process. Evolution of the WM is governed by the Markovian master equation in GKLS form derived microscopically for weak coupling and standard Born-Markov secular approximations [6],

$$\dot{\rho}_S(t) = -i[H_{\rm S}(\omega_B), \rho_S(t)] + \mathcal{D}_h[\rho_S(t)], \tag{6}$$

where $\mathcal{D}_h$ is the dissipative superoperator. After a sufficiently long time $\tau_h \gg \tau_B$ (bath correlation time), the WM is equilibriated with the bath with state $\rho_S^C = e^{-\beta_h H_{\rm S}(\omega_B)}/{\rm Tr}[e^{-\beta_h H_{\rm S}(\omega_B)}]$. Due to the weak coupling approximation, the joint system-bath state is always in the form $\rho_{\rm tot}(t) = \rho_S(t) \otimes \rho_B^i$ $(i = h, c)$.

Third stroke. Similar to the first stroke, this is the second unitary stroke, where the Hamiltonian is changed back from $H_{S,C} = H(\omega_B)$ to $H_{S,D} = H(\omega_A)$ in a time interval τ_{u2}. The final state of the working medium after the first unitary stroke is

$$\rho_S^D = U_2 \rho_S^C U_2^\dagger, \tag{7}$$

where $U_2 = \mathcal{T} \exp[-i\int_{t_C}^{t_D} H_{\rm S}(\omega(t))dt]$ is the unitary operator.

Fourth stroke. This is the second thermalization stroke, where the WM is connected to the cold bath at inverse temperature β_c, keeping the Hamiltonian fixed at $H_{\rm S}(\omega_A)$. If the stroke duration τ_c is sufficiently long ($\tau_c \gg \tau_B$), the WM is

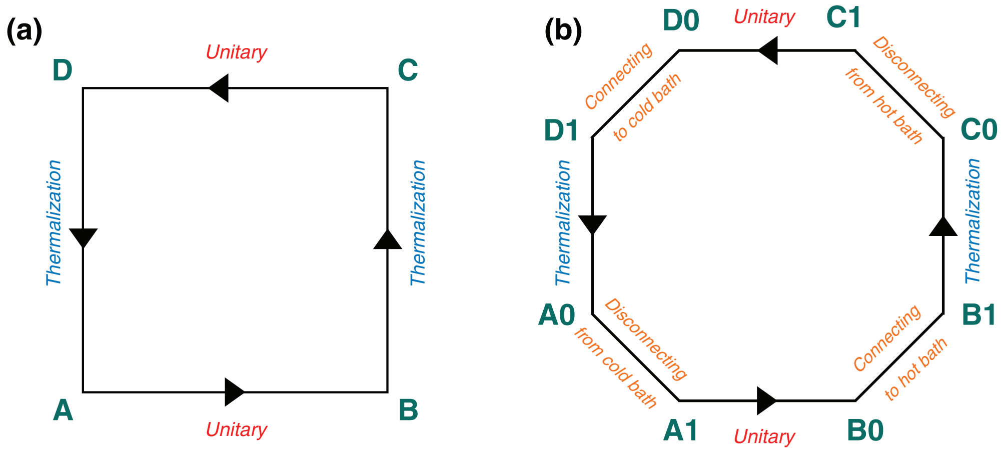

FIG. 1. Schematic of Otto cycle for (a) weak and (b) strong coupling.

returned to the initial thermal state $\rho_S^D = \rho_S^A$ completing the cycle.

Total cycle time is given by $\tau = \tau_{u1} + \tau_h + \tau_{u2} + \tau_c$. The definition of heat and work is well defined in the regime of weak interaction, given by, respectively [28,29],

$$\mathcal{Q} = \int \mathrm{Tr}[\dot{\rho}_S(t) H_S(t)]dt, \quad \mathcal{W} = \int \mathrm{Tr}[\rho_S(t)\dot{H}_S(t)]dt. \tag{8}$$

We now consider a specific model where the Hamiltonian of the WM is given as

$$H_S(t) = \omega(t)\sigma_z. \tag{9}$$

As mentioned before, $\omega(t)$ is the external parameter, which is changed from $\omega_A = \omega_c$ to $\omega_B = \omega_h$ in the first unitary stroke and back to ω_c in the final unitary stroke. Two thermal baths are always in usual equilibrium states with inverse temperatures β_h and $\beta_c(\beta_h < \beta_c)$, respectively. We calculate the heat and work done in each stroke for this model. Note that in the unitary strokes no heat is exchanged and in the thermalization strokes no work is done, as the Hamiltonian is kept fixed. Defining the average energy of the WM at the αth ($\alpha = A, B, C, D$) point as $E_\alpha = \mathrm{Tr}[\rho_S^\alpha H_{S,\alpha}]$, we get the following expressions for work and heat in different strokes:

$$\mathcal{W}_{AB}^0 = \langle E_B\rangle - \langle E_A\rangle = (\omega_c - \omega_h)\tanh\beta_c\omega_c, \tag{10}$$

$$\mathcal{Q}_h^0 = \langle E_C\rangle - \langle E_B\rangle = \omega_h(\tanh\beta_c\omega_c - \tanh\beta_h\omega_h), \tag{11}$$

$$\mathcal{W}_{CD}^0 = \langle E_D\rangle - \langle E_C\rangle = (\omega_h - \omega_c)\tanh\beta_h\omega_h, \tag{12}$$

$$\mathcal{Q}_c^0 = \langle E_A\rangle - \langle E_D\rangle = \omega_c(\tanh\beta_h\omega_h - \tanh\beta_c\omega_c). \tag{13}$$

It is evident from the above expressions that $\mathcal{W}_{AB}^0 + \mathcal{W}_{CD}^0 = -(\mathcal{Q}_h^0 + \mathcal{Q}_c^0)$, which is nothing but the energy conservation or the first law of thermodynamics. When $\omega_h/\omega_c > \beta_c/\beta_h$, the cycle works as a heat engine and we get the following expression for the power $\mathcal{P}_0$ as

$$\mathcal{P}_0 = -\frac{\mathcal{W}}{\tau} = -\frac{\mathcal{W}_{AB}^0 + \mathcal{W}_{CD}^0}{\tau} = \frac{\mathcal{Q}_h + \mathcal{Q}_c}{\tau} \tag{14}$$

and efficiency η_0 as

$$\eta_0 = -\frac{\mathcal{W}}{\mathcal{Q}_h^0} = -\frac{\mathcal{W}_{AB}^0 + \mathcal{W}_{CD}^0}{\mathcal{Q}_h^0} = 1 - \frac{\omega_c}{\omega_h}. \tag{15}$$

Similarly, in the refrigerator regime that is when $\omega_h/\omega_c < \beta_c/\beta_h$, and the cooling rate κ_0 is given as

$$\kappa_0 = \frac{\mathcal{Q}_c^0}{\tau}, \tag{16}$$

and the coefficient of performance K_0 is given as

$$K_0 = \frac{\mathcal{Q}_c^0}{\mathcal{W}_{AB}^0 + \mathcal{W}_{CD}^0} = \frac{\omega_c}{\omega_h - \omega_c}. \tag{17}$$

Here, we have used the sign convention that energy flow (heat, work) is positive (negative) if it enters (leaves) the WM. Hence a heat engine (refrigerator) is characterized by $\mathcal{Q}_h > 0$ (<0), $\mathcal{Q}_c < 0$ (>0), and $\mathcal{W} < 0$ (>0). The second law of thermodynamics gives us the bound on efficiency (coefficient of performance) for the engine (refrigerator). It states that the total entropy production is never negative. Now, for each separate thermalization stroke one has [28,80]

$$\Delta S_{\mathrm{tot}} = \Delta S - \beta\Delta Q \geqslant 0, \tag{18}$$

where ΔS is the change in the von Neumann entropy [81] of the system in a thermodynamic process, and ΔQ is the heat entering to the system form a bath at inverse temperature β. In our model of Otto cycle, one can check that $\rho_S^B = \rho_S^A$ and $\rho_S^C = \rho_S^D$. Hence, change in the von Neumann entropy of the system in the two thermalization strokes cancel each other and second law takes the form

$$\beta_h\mathcal{Q}_h^0 + \beta_c\mathcal{Q}_c^0 \leqslant 0, \tag{19}$$

as, of course, ΔS_{tot} remains zero in the unitary processes. The validity of the above inequality can easily be seen from the expressions of Eqs. (10)–(13) and employing the fact that $\tanh x$ is a monotonically increasing function of x. This implies that

$$\eta_0 = 1 + \frac{\mathcal{Q}_c^0}{\mathcal{Q}_h^0} = 1 - \frac{\omega_c}{\omega_h} \leqslant 1 - \frac{\beta_h}{\beta_c}. \tag{20}$$

Similarly, in the refrigerator regime, $K_0 \leqslant \frac{\beta_h}{\beta_c - \beta_h}$. This limit is famously known as the Carnot limit.

III. STRONGLY COUPLED OTTO CYCLE

In the strongly coupled model of the Otto cycle, the descriptions of the strokes are the same as in the weakly coupled one. Differences will come only in the thermodynamic framework. In this case, the thermalization stroke will make the system-bath joint state a correlated one, and the marginal bath state will no longer be a equilibrium state. Consequently, the thermodynamic analysis will change and we have to adopt different definitions of the thermodynamic observables suited for strongly coupled scenario. Here we follow the framework of Refs. [36,37,42] to define the thermodynamic quantities.

A. Formalism

Let us start by giving a short account of this framework. We first write the total Hamiltonian of a system-bath setup as follows:

$$H_{\text{tot}}(t) = H_{\text{S}}(t) + H_{\text{B}} + H_{\text{SB}}(t). \tag{21}$$

Change in average energy of the joint system-bath state is identified as the work performed,

$$dW(t) = dE_{\text{SB}}(t) = \text{Tr}[dH_{\text{tot}}(t)\rho_{SB}(t) + H_{\text{tot}}(t)d\rho_{SB}(t)], \tag{22}$$

where $E_{\text{SB}}(t) = \text{Tr}[\rho_{SB}(t)H_{\text{tot}}]$ is the total energy of the joint state $\rho_{SB}(t)$ of the system and bath. Heat is defined as the energy flowing out of the reservoir,

$$dQ(t) = -d\text{Tr}_B[H_{\text{B}}\rho_B(t)] = -\text{Tr}_B[H_{\text{B}}d\rho_B(t)] \tag{23}$$

$$= \text{Tr}[(H_{\text{S}}(t) + H_{\text{SB}}(t))d\rho_{SB}(t)], \tag{24}$$

where $\rho_B(t) = Tr_S[\rho_{SB}(t)]$. The internal energy of the system is defined as

$$E_{\text{S}}(t) = Tr_{SB}[(H_{\text{S}}(t) + H_{SB}(t))\rho_{SB}(t)]. \tag{25}$$

Now, it is easy to see that

$$dE_{\text{S}}(t) = dW(t) + dQ(t), \tag{26}$$

which is nothing but the first law of thermodynamics. In the weak coupling limit ($H_{\text{SB}} \approx 0$), these definitions boil down to the conventional definitions stated in the previous section. Let us assume the initial joint state as

$$\rho_{SB}(0) = \rho_S(0) \otimes \rho_B^{\beta}, \tag{27}$$

where ρ_B^{β} is the thermal state of the bath with inverse temperature β. The state of the joint system-bath setup at time $t = \tau$ is given by

$$\rho_{SB}(t) = U(\tau, 0)\rho_{SB}(0)U^{\dagger}(\tau, 0), \tag{28}$$

where $U(\tau, 0)$ is the unitary generated by the total Hamiltonian $H_{\text{tot}}(t)$. As mentioned before, entropy production is defined as $\Delta S_{\text{tot}} = \Delta S - \beta\Delta Q$. Note that β is the initial temperature of the bath. At later times, the reduced state of the bath is not even a thermal state. It can be shown that [36,42]

$$\Delta S_{\text{tot}}(t) = S\big[\rho_{SB}(t) \parallel \rho_S(t) \otimes \rho_B^{\beta}\big] \geqslant 0, \tag{29}$$

where $S(\phi \parallel \psi)$ is the relative entropy between two quantum states ϕ and ψ. This shows the validity of the second law of thermodynamics in this formalism. Next we derive the master equation used to describe the dynamics in our model of Otto cycle.

B. Dynamics with single qubit bath

We consider a two-qubit total Hamiltonian which can be considered as the total Hamiltonian of the system-bath setup,

$$\begin{aligned} H_{\text{tot}}(t) &= H_{\text{S}} \otimes \mathbb{1} + \mathbb{1} \otimes H_{\text{B}} + H_{\text{SB}}(t) \\ &= \omega(\sigma_z \otimes \mathbb{1} + \mathbb{1} \otimes \sigma_z) + H_{\text{SB}}(t), \end{aligned} \tag{30}$$

where the system Hamiltonian is $H_{\text{S}} = \omega\sigma_z$, bath Hamiltonian is $H_{\text{B}} = \omega\sigma_z$, and the interaction Hamiltonian $H_{\text{SB}}(t)$ reads

$$H_{\text{SB}}(t) = \frac{f(t)}{2}(\sigma_x \otimes \sigma_x + \sigma_y \otimes \sigma_y), \tag{31}$$

where $f(t)$ is a time-dependent coupling strength. The matrix form representation reads

$$H_{\text{SB}}(t) = \begin{bmatrix} 0 & 0 & 0 & 0 \\ 0 & 0 & f(t) & 0 \\ 0 & f(t) & 0 & 0 \\ 0 & 0 & 0 & 0 \end{bmatrix}. \tag{32}$$

Note here that we have chosen H_{S} and H_{B} in such a way in Eq. (30) that $H_{\text{tot}}(t)$ is different time commuting. Here, by different time commuting we mean $[H_{\text{tot}}(t), H_{\text{tot}}(t')] = 0$ for all $t \neq t'$, and as a result, the evolution operator as given in Eq. (34) can be calculated without considering time ordering [82]. We have also chosen this special form for the Hamiltonian so that for a specific choice of $f(t)$ (as discussed later) the system evolution will be described by a semigroup master equation [6,79]. Not only that, we can also smoothly transit to the non-Markovian regime by changing the form of $f(t)$. Now we choose the initial states of the system and environment to be

$$\rho_{\text{S}}(0) = \begin{bmatrix} p & x \\ x^* & 1-p \end{bmatrix}, \quad \rho_{\text{B}}(0) = \frac{1}{2}\begin{bmatrix} 1-g & 0 \\ 0 & 1+g \end{bmatrix}, \tag{33}$$

where $0 \leqslant p, g \leqslant 1$, and x is a complex number with $|x|^2 \leqslant p(1-p)$. One can assign a temperature to the initial bath state with respect to the bath Hamiltonian H_{B} to write it as a thermal state. The initial joint system-bath state $\rho_{SB}(0) = \rho_{\text{S}}(0) \otimes \rho_{\text{B}}(0)$ evolves through the unitary:

$$U(t, 0) = \exp\left[-i\int_0^t dt'\, H_{\text{tot}}(t')\right]. \tag{34}$$

Note here that we have used the fact that $H_{\text{tot}}(t)$ is different time commuting. A quantum circuit realization of $U(t, 0)$ is given in Fig. 2 [83,84]. One finds that $U(t, 0)$ can be realized

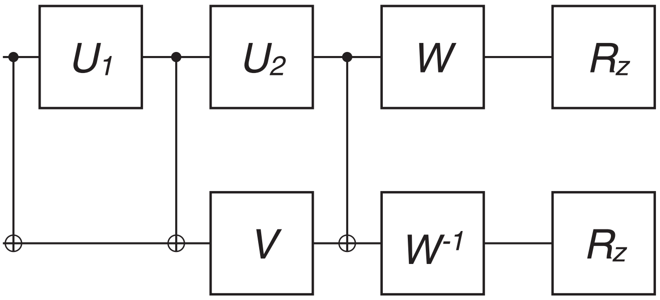

FIG. 2. Circuit realization of $U(t,0)$ as given in Eq. (34).

as the following composition of qubit gates:

$$U(t,0)=\mathrm{CNOT}[U_1(t)\otimes\mathbb{1}]\,\mathrm{CNOT}[U_2\otimes V(t)]\times\mathrm{CNOT}[W\otimes W^{-1}][R_z(t)\otimes R_z(t)],\tag{35}$$

where

$$U_1(t)=\frac{i}{\sqrt{2}}(\sigma_x+\sigma_z)\,e^{-i(\frac{F(t)}{2}-\frac{\pi}{4})\sigma_x},\tag{36}$$

$$U_2=\frac{-i}{\sqrt{2}}(\sigma_x+\sigma_z),\tag{37}$$

$$\mathrm{CNOT}=|0\rangle\langle 0|\otimes\mathbb{1}+|1\rangle\langle 1|\otimes\sigma_x,\tag{38}$$

and diagonal unitaries

$$V(t)=e^{i\frac{F(t)}{2}\sigma_z}\,,\quad W=\frac{\mathbb{1}-i\sigma_z}{\sqrt{2}}\,,\quad R_z=e^{-i\omega t\,\sigma_z}.$$

The time-evolved system state is $\rho_S(t)=\mathrm{Tr}_B[\rho_{SB}(t)]$, where $\rho_{SB}(t)=U(t,0)\rho_{SB}(0)U^\dagger(t,0)$. The explicit form of ρ_S can be written as

$$\rho_S(t)=\Lambda_t[\rho_S(0)]=\begin{bmatrix}p(t) & xe^{-2i\omega t}\cos F(t)\\ x^*e^{2i\omega t}\cos F(t) & 1-p(t)\end{bmatrix},\tag{39}$$

where

$$p(t)=p\cos^2F(t)+\frac{1-g}{2}\sin^2F(t),$$

Λ_t is the dynamical map, and $F(t)=\int_0^t f(t')\,dt'$. The corresponding master equation

$$\frac{d\rho_S}{dt}=\mathcal{L}_t[\rho_S]\tag{40}$$

reads as follows (cf. Appendix B):

$$\begin{aligned}\frac{d\rho_S(t)}{dt}&=-i\omega[\sigma_z,\rho_S(t)]\\&\quad+\gamma_-(t)\big(\sigma_-\rho_S(t)\sigma_+-\tfrac{1}{2}\{\sigma_+\sigma_-,\rho_S(t)\}\big)\\&\quad+\gamma_+(t)\big(\sigma_+\rho_S(t)\sigma_--\tfrac{1}{2}\{\sigma_-\sigma_+,\rho_S(t)\}\big),\end{aligned}\tag{41}$$

with

$$\gamma_\pm(t)=(1\mp g)\gamma(t)\tag{42}$$

and

$$\gamma(t)=f(t)\tan F(t).\tag{43}$$

It is therefore clear that the evolution is Markovian (CP divisible) if [10,85,86]

$$\gamma(t)\geqslant 0.\tag{44}$$

We can choose $f(t)$ in a form such that $\cos F(t)\to 0$ as $t\to\infty$. In that case the system state asymptotically approaches the initial bath state, which can be seen as thermalization. Interestingly, one can show [79] that choosing $f(t)$,

$$f(t)=\frac{e^{-t/2g}}{2g\sqrt{1-e^{-t/g}}},\tag{45}$$

leads to $\gamma(t)=\frac{1}{2g}$, and hence both rates,

$$\gamma_-=\tfrac{1+g}{2g},\quad \gamma_+=\tfrac{1-g}{2g},$$

are time independent, leading to the GKLS Markovian master equation. In this case the asymptotic state of the system is a thermal state in the following form:

$$\rho_S(t\to\infty)=\frac{1}{2}\begin{bmatrix}1-g & 0\\ 0 & 1+g\end{bmatrix}.\tag{46}$$

Later we also discuss non-Markovian generalization of the master equation in Eq. (41) with other choices of $f(t)$.

C. Implementation of the Otto cycle

In this section we implement an Otto cycle where the WM is connected to two single-qubit baths (hot and cold). Dynamics in the thermalization strokes is described by the formalism developed upstairs. For the sake of clarity of notation, we will append all the relevant quantities in the single-qubit bath, namely, Hamiltonians, ω, g, $f(t)$ and $F(t)$, with a suffix h or c depending on whether it is used in connection with the hot bath or the cold bath, respectively. The total Hamiltonians of the WM and the baths are described as

$$H(t)=H_\mathrm{S}(t)+H_{\mathrm{B_h}}+H_{\mathrm{B_c}}+H_\mathrm{SB}(t),\tag{47}$$

where $H_\mathrm{S}(t)=\omega(t)\sigma_z$. The external parameter $\omega(t)$ is varied from ω_c to ω_h in the first unitary stroke and changed back to ω_c in the second unitary stroke. $H_{\mathrm{B_h}}$ and $H_{\mathrm{B_c}}$ are $\omega_h\sigma_z$ and $\omega_c\sigma_z$, in accordance with Eq. (30). The interaction Hamiltonian $H_\mathrm{SB}(t)=H^h_\mathrm{SB}(t)+H^c_\mathrm{SB}(t)$ is given as Eq. (32), with prefix h and c for $f(t)$ the contact with the hot and cold bath, respectively. The initial states of the hot and cold baths are as follows:

$$\begin{aligned}\rho_{\mathrm{B_h}}(0)&=\frac{1}{2}\begin{bmatrix}1-g_h & 0\\ 0 & 1+g_h\end{bmatrix},\\ \rho_{\mathrm{B_c}}(0)&=\frac{1}{2}\begin{bmatrix}1-g_c & 0\\ 0 & 1+g_c\end{bmatrix}.\end{aligned}\tag{48}$$

Initial temperatures of the baths can be determined by writing the states in the form of thermal states,

$$\rho_{\mathrm{B_j}}(0)=\frac{e^{-\beta_jH_{\mathrm{B_j}}}}{Z_j},\quad j=\{h,c\},\tag{49}$$

where $Z_j=\mathrm{Tr}[e^{-\beta_jH_{\mathrm{B_j}}}]$, which gives us $g_h=\tanh\beta_h\omega_h$, and similarly, $g_c=\tanh\beta_c\omega_c$. Below we describe the strokes of the cycle. The schematic of the cycle is shown in Fig. 1(b).

WM is initially (point A1) prepared in the thermal state corresponding to the initial temperature of the cold bath, and the total WM-bath state is prepared initially in a product state as follows:

$$\rho_{\rm tot}^{A} = \frac{e^{-\beta_c H_{\rm S}(\omega_c)}}{\mathrm{Tr}[e^{-\beta_c H_{\rm S}(\omega_c)}]} \otimes \frac{e^{-\beta_c H_{\rm B_c}}}{\mathrm{Tr}[e^{-\beta_c H_{\rm B_c}}]}, \tag{50}$$

where the initial state of the cold bath in Eq. (48) is written in the form of Eq. (49). Below we describe the strokes of the Otto cycle.

First stroke. In the first unitary stroke, WM is disconnected from the baths and the external parameter $\omega(t)$ of the system Hamiltonian is varied from ω_c (point $A1$) to ω_h (point $B0$) in a time interval τ_{u1}. The state does not change during the evolution and remains constant at $\rho_S^{A1} = e^{-\beta_c H_{\rm S}(\omega_c)}/Z_c$, where $Z_c = \mathrm{Tr}[\mathrm{e}^{-\beta_c \mathrm{H_S}(\omega_c)}]$. No heat is exchanged in this process, whereas the work done is given by

$$\mathcal{W}_{AB} = \langle E_S^{B0}\rangle - \langle E_S^{A1}\rangle = (\omega_c - \omega_h)\tanh\beta_c\omega_c. \tag{51}$$

Here, $E_S^{\alpha} = \mathrm{Tr}[\rho_S^{A1} H_{\rm S}(\omega_\alpha)]$, with $\alpha = \{h, c\}$.

Connecting the hot bath. The WM is connected to the hot bath as represented by point $B0$ to $B1$ in the schematic diagram [Fig. 1(b)]. We assume that this coupling operation is instantaneous. Hence the state of the WM and the bath do not change during this operation. Additionally, the interaction Hamiltonian also remains constant. As a result, the energy change of the total WM-bath setup during this operation is

$$\mathcal{W}_B^{\rm con} = \mathrm{Tr}\big[H_{\rm SB}^h(0)(\rho_{\rm B_h}(0)\otimes e^{-\beta_c H_{\rm S}(\omega_c)}/Z_c)\big] = 0,$$

where $\rho_{\rm B_h}(0)$ is as given in Eq. (48), with $g_h = \tanh\beta_h\omega_h$, and $H_{\rm SB}^h(0)$ is given as Eq. (32) with the parameter as $f^h(0)$. A functional form of $f^j(t)$ for $j = \{h, c\}$ will be specified later for both a Markovian and non-Markovian scenario.

Second stroke. The second stroke is the thermalization stroke after the WM is connected to the hot bath. As the state of the bath does not change during the connection of WM to it, at the start of the stroke, its state is given by $\rho_{\rm B_h}(0)$. We assume that the WM is kept in contact with the bath for a time interval τ_h ($B1$ to $C0$ in the schematic), keeping the system Hamiltonian constant at $H_{\rm S}(\omega_h)$. Work done in this process is zero, as calculated using Eq. (22). Using the definition in Eq. (24), heat exchanged in this stroke is given as

$$\begin{aligned}\mathcal{Q}_h = \mathcal{Q}_{BC} &= \int_0^{\tau_h} dt\ \mathrm{Tr}\bigg[\big[\omega_h\sigma_z + H_{\rm SB}^h(t)\big]\frac{d}{dt}\rho_{\rm tot}(t)\bigg]\\ &= \omega_h(\tanh\beta_c\omega_c - \tanh\beta_h\omega_h)\sin^2 F^h(\tau_h)\\ &= \mathcal{Q}_h^0 \sin^2 F^h(\tau_h).\end{aligned} \tag{52}$$

Here $F^h(\tau_h) = \int_0^{\tau_h} f^h(t)dt$, and $\mathcal{Q}_h^0$ is the heat exchanged in the weakly coupled Otto cycle (assuming the WM is thermalized at the end of the stroke), given as Eq. (11). After the thermalization stroke, the total state of the WM-bath setup is $\rho_{\rm tot}^{C0}$, which is in general a correlated state. The reduced state of the WM denoted by ρ_S^{C0} will be in the form of Eq. (39), with $x = 0$, and p to be the initial population of the WM before the start of the stroke. Note here that the heat exchange $\mathcal{Q}_h$ can be alternatively calculated from the formula given in Eq. (23), where in this case the time-evolved bath state is given by (see Appendix A)

$$\rho_B(t) = \begin{bmatrix} q(t) & 0\\ 0 & 1-q(t)\end{bmatrix}, \tag{53}$$

where $q(t) = \frac{1-g}{2}\cos^2 F^h(t) + p\sin^2 F^h(t)$.

Disconnecting the hot bath. The work done to remove the bath is given by

$$\mathcal{W}_C^{\rm discon} = -\mathrm{Tr}\big[H_{\rm SB}^h(\tau_h)\ \rho_{\rm tot}^{C0}\big] = 0, \tag{54}$$

where we again assumed the process is instantaneous and denoted from the point $C0$ to $C1$ in Fig. 1.

Third stroke. This is the second and final unitary stroke, which is represented from point $C1$ to $D0$ in the schematic [Fig. 1(b)], taking place in the time interval τ_{u2}. The WM is disconnected from the bath, and the system Hamiltonian is changed back from $H_{\rm S}(\omega_h)$ to $H_{\rm S}(\omega_c)$. The reduced state of the WM at the start of this stroke is given as

$$\rho_S^{C1} = \begin{bmatrix} p^{C1} & 0\\ 0 & 1-p^{C1}\end{bmatrix}, \tag{55}$$

where $p^{C1} = \frac{e^{-\beta_h\omega_h}}{Z_h} + \frac{\cos^2 F^h(\tau_h)}{2}(g_h - g_c)$. Here $Z_h = \mathrm{Tr}[e^{-\beta_h H_{\rm S}(\omega_h)}]$. The reduced state of the WM will not change during the unitary evolution. The work done in this stroke is thus

$$\begin{aligned}\mathcal{W}_{CD} &= \langle E_{D0}\rangle - \langle E_{C1}\rangle = (\omega_c - \omega_h)\mathrm{Tr}\big[\sigma_z\,\rho_S^{C1}\big]\\ &= (\omega_h - \omega_c)[g_h - \cos^2 F^h(\tau_h)(g_h - g_c)],\end{aligned} \tag{56}$$

where $g_h = \tanh\beta_h\omega_h$ and $g_c = \tanh\beta_c\omega_c$ as mentioned before.

Connecting the cold bath. Similarly as before, the process [from $D0$ to $D1$ in Fig. 1(b)] is instantaneous and the work done in the process is

$$\mathcal{W}_D^{\rm con} = \mathrm{Tr}\big[H_{\rm SB}^c(0)(\rho_S^{C1}\otimes\rho_{\rm B_c}(0))\big] = 0. \tag{57}$$

Here $\rho_{\rm B_c}(0)$ is as given in Eq. (48), with $g_c = \tanh\beta_c\omega_c$, and $H_{\rm SB}^c(0)$ is given as Eq. (32), with the parameter denoted as $f^c(0)$.

Fourth stroke. This is the second and final thermalization stroke denoted from $D1$ to $A0$ in the schematic [Fig. 1(b)]. After connecting the the WM to the cold bath, it is kept in contact for a time interval τ_c. Work done is again zero for this stroke. Using the definition in Eq. (24), heat exchange is calculated to be

$$\begin{aligned}\mathcal{Q}_c = \mathcal{Q}_{DA} &= \int_0^{\tau_c} dt\mathrm{Tr}\bigg[(\omega_c\sigma_z + H_{\rm SB}^c(t))\frac{d}{dt}\rho_{\rm tot}(t)\bigg]\\ &= \omega_c(\tanh\beta_h\omega_h - \tanh\beta_c\omega_c)\sin^2 F^h(\tau_h)\sin^2 F^c(\tau_c)\\ &= \mathcal{Q}_c^0\sin^2 F^h(\tau_h)\sin^2 F^c(\tau_c),\end{aligned} \tag{58}$$

where $\mathcal{Q}_c^0$ is the heat exchanged in the weakly coupled Otto cycle (assuming the WM is thermalized at the end of the stroke). At the end of this stroke, state of the total WM-bath setup is $\rho_{\rm tot}^{A0}$, which is again correlated in general.

Disconnecting the cold bath. In the last step, the cold bath is disconnected from the WM instantaneously [shown as $A0$ to $A1$ in Fig. 1(b)]. Similarly as before, the work done in this process is also zero:

$$\mathcal{W}_A^{\rm discon} = -\mathrm{Tr}\big[H_{\rm SB}^c(\tau_c)\ \rho_{\rm tot}^{A0}\big] = 0. \tag{59}$$

In general, the work cost for connecting and disconnecting the baths with WM is not free [62,63]. But for our special kind of model the cost turns out to be zero.

Now, total work done in the cycle is given by $\mathcal{W} = \mathcal{W}_{AB} + \mathcal{W}_{CD}$, which is

$$\begin{aligned}\mathcal{W} &= (\omega_c - \omega_h)(\tanh \beta_c\omega_c - \tanh \beta_h\omega_h)\sin^2 F^h(\tau_h)\\ &= \mathcal{W}_0 \sin^2 F^h(\tau_h).\end{aligned} \tag{60}$$

Here $\mathcal{W}_0$ is the total work done in the weakly coupled Otto cycle. Thus for the heat engine regime, we find the expression for power and efficiency as

$$\mathcal{P} = -\frac{\mathcal{W}}{\tau} = \mathcal{P}_0 \sin^2 F^h(\tau_h), \quad \text{and} \quad \eta = -\frac{\mathcal{W}}{\mathcal{Q}_h} = \eta_0, \tag{61}$$

where $\mathcal{P}_0$ and η_0 are the power and efficiency for the weakly coupled Otto cycle in the previous section. Interestingly, for this particular model we notice that the efficiency is always the same as the maximal efficiency of the weakly coupled counterpart irrespective of the power. The cost we pay for this advantage is that after one cycle the state of the bath does not return to its initial states, whereas to reach maximum efficiency in the case of the weakly coupled Otto engine, we need perfect thermalizations in the nonunitary strokes. For the refrigerator regime, the expressions for cooling rate and CoP are as follows:

$$\kappa = \frac{\mathcal{Q}_c}{\tau} = \kappa_0 \sin^2 F^h(\tau_h)\sin^2 F^c(\tau_c), \tag{62}$$

$$K = \frac{\mathcal{Q}_c}{\mathcal{W}} = K_0 \sin^2 F^c(\tau_c). \tag{63}$$

Notably, for the refrigerator regime, the coefficient of performance is dependent on the last thermalization stroke. In the next section we show that with perfect thermalization in the last unitary stroke $\sin^2 F^c(\tau_c) = 1$, we achieve the maximum coefficient of performance in the strongly coupled Otto cycle too.

D. Markovian and non-Markovian scenario

Depending upon the functional form of $f(t)$, one can make the system dynamics Markovian or non-Markovian. Note here that we must choose $f(t)$ such that the thermalizing condition is obeyed, i.e., $\cos F(t) \to 0$ as $t \to \infty$.

Let us first recall the form of $f(t)$ given in Eq. (45):

$$f(t) = \frac{e^{-t/2g}}{2g\sqrt{1 - e^{-t/g}}}. \tag{64}$$

As a result we get $F(t) = \frac{\pi}{2} - \sin^{-1} e^{-t/2g}$, which gives us $f(t)\tan F(t) = 1/2g \geqslant 0$ for all $t > 0$ and the corresponding master equation as a semigroup master equation. Hence, from Eq. (44) we find that the dynamics is Markovian. From Eq. (39) one can further note that in the long time limit ($t \to \infty$) compared to the bath correlation time, the initially diagonal system state in the σ_z basis approaches the fixed thermal state. This shows that indeed our model achieves thermalization. Now, it is straightforward to notice that $\sin^2 F(t) = 1 - e^{-t/g}$ if τ is the time taken for the thermalization strokes. So, on applying to the Otto cycle we get

$$K = K_0(1 - e^{-\tau_c/g_c}). \tag{65}$$

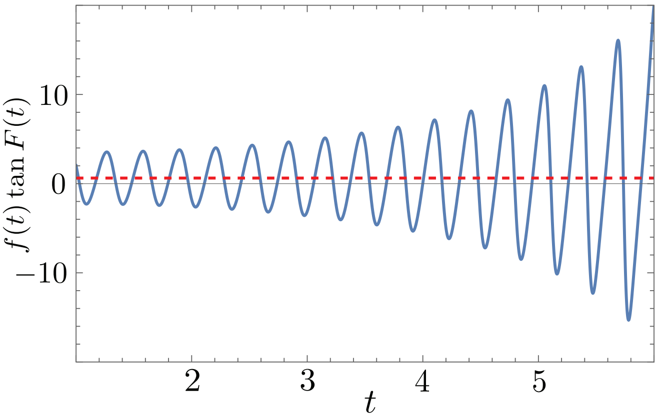

FIG. 3. Plot of $f(t)\tan F(t)$ vs t for Markovian (red dashed) and non-Markovian (solid blue) dynamics with $g = 0.8$.

For perfect thermalization to occur in the last nonunitary stroke, in principle we need $\tau_c \to \infty$ (in the scale of bath correlation time). This shows that we can get the maximum achievable coefficient of performance in the strongly coupled scenario. In this case we also notice that $\mathcal{W} = -(\mathcal{Q}_h + \mathcal{Q}_c)$, which is nothing but the first law of thermodynamics for a complete cycle. This justifies the consistency of our thermodynamic framework.

We now choose the following form of $f(t)$, which gives a non-Markovian dynamics according to the condition of Eq. (44). It can be thought of as a non-Markovian correction to the previous form of $f(t)$:

$$f(t) = \frac{e^{-t/2g}}{2g\sqrt{1 - e^{-t/g}}} - \frac{10\sin(20t)}{(10t+1)^2} + \frac{20\cos(20t)}{10t+1}. \tag{66}$$

One can easily check whether this functional form gives rise to non-Markovian dynamics. In Fig. 3 we plot $f(t)\tan F(t)$ with t, whose non-negativity ensures Markovian dynamics. It is evident from the plot that for the second form of $f(t)$ the condition breaks down, resulting a non-Markovian dynamics, whereas for the first form $f(t)\tan F(t)$ is always positive. Again, from Eq. (39) one can check that in the limit of $t \to \infty$, initially the diagonal system state in σ_z basis

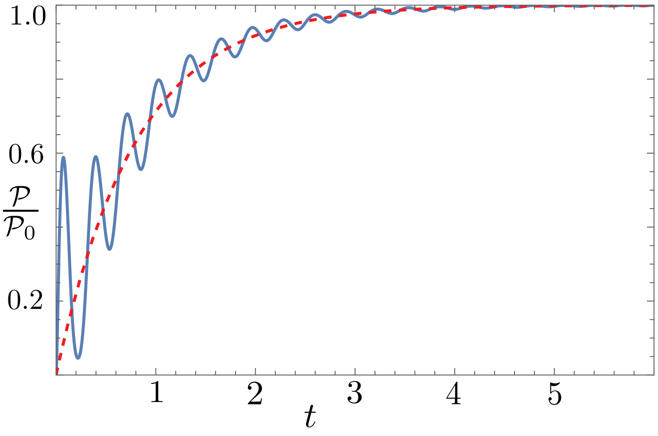

FIG. 4. Plot of $\mathcal{P}/\mathcal{P}_0$ vs t for Markovian (red dashed) and non-Markovian (solid blue) dynamics with $g = 0.8$.

thermalizes for the non-Markovian form of $f(t)$ also. In Fig. 4 we plot $\sin^2 F(t)$ with t for $g = 0.8$ to show the non-Markovian advantage for power output in the Otto engine. Clearly, the oscillatory behavior of $\sin^2 F(t)$ for the non-Markovian scenario gives an enhancement over the Markovian scenario, as evident from the expression of power as $\mathcal{P} = \mathcal{P}_0 \sin^2 F^h(\tau)$. With increasing time, both reach the limit $\mathcal{P}_0$ of the weakly coupled Otto engine. Similarly, for the Otto refrigerator one can see a similar kind of behavior.

IV. CONCLUSION

In this paper we have studied a quantum Otto cycle model with a single qubit bath. First, from a closed quantum evolution of two qubits with a specially chosen joint Hamiltonian, we derive an exact master equation for a single qubit in the form of a semigroup master equation. By tweaking the form of the joint Hamiltonian, one can end up with both Markovian and non-Markovian dynamics. Next we construct an Otto cycle employing this dynamic in the thermalization strokes to investigate the thermodynamic implications of this model. Our model provides a link to study the interplay between strong coupling and non-Markovianity. We employ the formalism of strongly coupled quantum thermodynamics to calculate the thermodynamic quantities for the Otto cycle for both Markovian and non-Markovian scenarios. Interestingly, for the Otto engine we find that the efficiency is always maximal, irrespective of whether the WM is thermalized or partially thermalized in the nonunitary strokes, whereas for a refrigerator, perfect thermalization in the last stroke is needed to achieve the maximal coefficient of performance. On the other hand, with approximate thermalization, the power output is hampered in the strongly coupled Otto cycle. In this scenario we can exploit the non-Markovianity, which provides an enhancement of performance over the Markovian counterpart. In the long time limit, power output for both Markovian and non-Markovian models reaches the limit of a weakly coupled cycle. For an Otto refrigerator one can also see similar effects. It is important to note that the observations are based on the specific model we have chosen. This special model has enabled us to demonstrate the non-Markovian advantage for thermodynamic tasks, yet in the regime of strong coupling.

ACKNOWLEDGMENT

This work was supported by the Polish National Science Centre through Project No. 2018/30/A/ST2/00837. S.C. would like to acknowledge Sibasish Ghosh for useful discussions of the problem.

APPENDIX A

One finds the following formula for the time-evolved system-environment state:

$$\rho_{SB}(t) = \begin{pmatrix} \frac{1-g}{2}p & i\frac{1-g}{2}xe^{-2it\omega}\sin F(t) & \frac{1-g}{2}xe^{-2it\omega}\cos F(t) & 0 \\ -i\frac{1-g}{2}x^*e^{2it\omega}\sin F(t) & \frac{1-g}{2}\sin^2 F(t) + \frac{p}{2}(g+\cos 2F(t)) & \frac{i}{4}(g+2p-1)\sin 2F(t) & \frac{1+g}{2}xe^{-2it\omega}\cos F(t) \\ \frac{1-g}{2}x^*e^{2it\omega}\cos F(t) & -\frac{i}{4}(g+2p-1)\sin 2F(t) & \frac{1-g}{2}\cos^2 F(t) + \frac{p}{2}(g-\cos 2F(t)) & -i\frac{1+g}{2}xe^{-2it\omega}\sin F(t) \\ 0 & \frac{1+g}{2}x^*e^{2it\omega}\cos F(t) & i\frac{1+g}{2}x^*e^{2it\omega}\sin F(t) & \frac{1+g}{2}(1-p) \end{pmatrix}, \tag{A1}$$

which reduces to

$$\rho_{SB}(t) = \begin{pmatrix} \frac{1-g}{2}p & 0 & 0 & 0 \\ 0 & \frac{1-g}{2}\sin^2 F(t) + \frac{p}{2}(g+\cos 2F(t)) & \frac{i}{4}(g+2p-1)\sin 2F(t) & 0 \\ 0 & -\frac{i}{4}(g+2p-1)\sin 2F(t) & \frac{1-g}{2}\cos^2 F(t) + \frac{p}{2}(g-\cos 2F(t)) & 0 \\ 0 & 0 & 0 & \frac{1+g}{2}(1-p) \end{pmatrix}, \tag{A2}$$

for $x = 0$.

APPENDIX B

The dynamical map Λ_t and $\mathcal{L}_t$ as given in Eqs. (39) and (40) are given by the following matrices in the operator-vector correspondence representation [87] as

$$\hat{\Lambda}_t = \begin{bmatrix} 1 - \frac{1+g}{2}\sin^2 F(t) & 0 & 0 & \frac{1-g}{2}\sin^2 F(t) \\ 0 & e^{-2i\omega t}\cos F(t) & 0 & 0 \\ 0 & 0 & e^{2i\omega t}\cos F(t) & 0 \\ \frac{1+g}{2}\sin^2 F(t) & 0 & 0 & 1 - \frac{1-g}{2}\sin^2 F(t) \end{bmatrix}, \tag{B1}$$

$$\hat{\mathcal{L}}_t = \dot{\hat{\Lambda}}_t \circ \hat{\Lambda}_t^{-1} = \begin{bmatrix} -(1+g)\gamma(t) & 0 & 0 & (1-g)\gamma(t) \\ 0 & -2i\omega - \gamma(t) & 0 & 0 \\ 0 & 0 & 2i\omega - \gamma(t) & 0 \\ (1+g)\gamma(t) & 0 & 0 & -(1-g)\gamma(t) \end{bmatrix}. \tag{B2}$$

[1] J. P. Dowling and G. J. Milburn, Quantum technology: The second quantum revolution, Philos. Trans. R. Soc. A, **361**, 1655 (2003).

[2] D. A. Golter, T. Oo, M. Amezcua, K. A. Stewart, and H. Wang, Optomechanical Quantum Control of a Nitrogen-Vacancy Center in Diamond, Phys. Rev. Lett. **116**, 143602 (2016).

[3] N. Accanto, P. M. de Roque, M. Galvan-Sosa, S. Christodoulou, I. Moreels, and N. F. van Hulst, Rapid and robust control of single quantum dots, Light Sci. Appl. **6**, e16239 (2017).

[4] W. E. Perreault, N. Mukherjee, and R. N. Zare, Quantum control of molecular collisions at 1 kelvin, Science **358**, 356 (2017).

[5] M. Rossi, D. Mason, J. Chen, Y. Tsaturyan, and A. Schliesser, Measurement-based quantum control of mechanical motion, Nature (London) **563**, 53 (2018).

[6] H. P. Breuer and F. Petruccione, *The Theory of Open Quantum Systems* (Oxford University Press, Oxford, England, 2002).

[7] E. B. Davies, Markovian master equations, Commun. Math. Phys. **39**, 91 (1974).

[8] V. Gorini, A. Kossakowski, and E. C. G. Sudarshan, Completely positive dynamical semigroups of n-level systems, J. Math. Phys. **17**, 821 (1976).

[9] G. Lindblad, On the generators of quantum dynamical semigroups, Commun. Math. Phys. **48**, 119 (1976).

[10] Á. Rivas, S. F. Huelga, and M. B. Plenio, Quantum non-Markovianity: Characterization, quantification and detection, Rep. Prog. Phys. **77**, 094001 (2014).

[11] H.-P. Breuer, E.-M. Laine, J. Piilo, and B. Vacchini, Colloquium: Non-Markovian dynamics in open quantum systems, Rev. Mod. Phys. **88**, 021002 (2016).

[12] L. Li, M. J. W. Hall, and H. M. Wiseman, Concepts of quantum non-Markovianity: A hierarchy, Phys. Rep. **759**, 1 (2018).

[13] I. de Vega and D. Alonso, Dynamics of non-Markovian open quantum systems, Rev. Mod. Phys. **89**, 015001 (2017).

[14] D. Chruściński, Dynamical maps beyond Markovian regime, Phys. Rep. **992**, 1 (2022).

[15] S. Chakraborty and D. Chruściński, Information flow versus divisibility for qubit evolution, Phys. Rev. A **99**, 042105 (2019).

[16] D. Chruściński, A. Rivas, and E. Størmer, Divisibility and Information Flow Notions of Quantum Markovianity for Noninvertible Dynamical Maps, Phys. Rev. Lett. **121**, 080407 (2018).

[17] S. Chakraborty, Generalized formalism for information backflow in assessing Markovianity and its equivalence to divisibility, Phys. Rev. A **97**, 032130 (2018).

[18] B. Bylicka, M. Johansson, and A. Acín, Constructive Method for Detecting the Information Backflow of Non-Markovian Dynamics, Phys. Rev. Lett. **118**, 120501 (2017).

[19] F. A. Pollock, C. Rodríguez-Rosario, T. Frauenheim, M. Paternostro, and K. Modi, Operational Markov Condition for Quantum Processes, Phys. Rev. Lett. **120**, 040405 (2018).

[20] S. Milz, M. S. Kim, F. A. Pollock, and K. Modi, Completely Positive Divisibility Does Not Mean Markovianity, Phys. Rev. Lett. **123**, 040401 (2019).

[21] S. Milz and K. Modi, Quantum stochastic processes and quantum non-Markovian phenomena, PRX Quantum **2**, 030201 (2021).

[22] S. Milz, D. Egloff, P. Taranto, T. Theurer, M. B. Plenio, A. Smirne, and S. F. Huelga, When Is a Non-Markovian Quantum Process Classical? Phys. Rev. X **10**, 041049 (2020).

[23] C. W. Gardiner, P. Zoller, and P. Zoller, *Quantum Noise: A Handbook of Markovian and Non-Markovian Quantum Stochastic Methods with Applications to Quantum Optics* (Springer Science & Business Media, New York, 2004).

[24] H. Carmichael, *An Open Systems Approach to Quantum Optics: Lectures Presented at the Université Libre de Bruxelles, October 28 to November 4, 1991* (Springer Science & Business Media, New York, 2009), Vol. 18.

[25] D. Lonigro and D. Chruściński, Quantum regression beyond the born-Markov approximation for generalized spin-boson models, Phys. Rev. A **105**, 052435 (2022).

[26] R. Kosloff, Quantum thermodynamics: A dynamical viewpoint, Entropy **15**, 2100 (2013).

[27] *Thermodynamics in the Quantum Regime*, edited by F. Binder, L. A. Correa, C. Gogolin, J. Anders, and G. Adesso (Springer International Publishing, Cham, Switzerland, 2018).

[28] S. Vinjanampathy and J. Anders, Quantum thermodynamics, Contemp. Phys. **57**, 545 (2016).

[29] R. Alicki, The quantum open system as a model of the heat engine, J. Phys. A: Math. Gen. **12**, L103 (1979).

[30] R. Alicki and R. Kosloff, in *Introduction to Quantum Thermodynamics: History and Prospects. Thermodynamics in the Quantum Regime*, edited by F. Binder, L. A. Correa, C. Gogolin, J. Anders, and G. Adesso (Springer, Cham, Switzerland, 2019).

[31] R. Kosloff and A. Levy, Quantum heat engines and refrigerators: Continuous devices, Annu. Rev. Phys. Chem. **65**, 365 (2014).

[32] E. B. Davies and H. Spohn, Open quantum systems with time-dependent Hamiltonians and their linear response, J. Stat. Phys. **19**, 511 (1978).

[33] T. Albash, S. Boixo, D. A. Lidar, and P. Zanardi, Quantum adiabatic Markovian master equations, New J. Phys. **14**, 123016 (2012).

[34] I. Kamleitner, Secular master equation for adiabatically driven time-dependent systems, Phys. Rev. A **87**, 042111 (2013).

[35] M. Yamaguchi, T. Yuge, and T. Ogawa, Markovian quantum master equation beyond adiabatic regime, Phys. Rev. E **95**, 012136 (2017).

[36] M. Esposito, K. Lindenberg, and C. V. den Broeck, Entropy production as correlation between system and reservoir, New J. Phys. **12**, 013013 (2010).

[37] A. Kato and Y. Tanimura, Quantum heat current under non-perturbative and non-Markovian conditions: Applications to heat machines, J. Chem. Phys. **145**, 224105 (2016).

[38] P. Strasberg, G. Schaller, T. Brandes, and M. Esposito, Quantum and Information Thermodynamics: A Unifying Framework Based on Repeated Interactions, Phys. Rev. X **7**, 021003 (2017).

[39] M. Perarnau-Llobet, H. Wilming, A. Riera, R. Gallego, and J. Eisert, Strong Coupling Corrections in Quantum Thermodynamics, Phys. Rev. Lett. **120**, 120602 (2018).

[40] W. Dou, M. A. Ochoa, A. Nitzan, and J. E. Subotnik, Universal approach to quantum thermodynamics in the strong coupling regime, Phys. Rev. B **98**, 134306 (2018).

[41] P. Strasberg, Repeated Interactions and Quantum Stochastic Thermodynamics at Strong Coupling, Phys. Rev. Lett. **123**, 180604 (2019).

[42] A. Rivas, Strong Coupling Thermodynamics of Open Quantum Systems, Phys. Rev. Lett. **124**, 160601 (2020).

[43] N. Bergmann and M. Galperin, A Green's function perspective on the nonequilibrium thermodynamics of open quantum systems strongly coupled to baths, Eur. Phys. J.: Spec. Top. **230**, 859 (2021).

[44] H. J. D. Miller, Hamiltonian of mean force for strongly-coupled systems, in *Thermodynamics in the Quantum Regime: Fundamental Aspects and New Directions*, edited by F. Binder, L. A. Correa, C. Gogolin, J. Anders, and G. Adesso (Springer International Publishing, Cham, Switzerland, 2018), pp. 531–549.

[45] A. Nazir and G. Schaller, The reaction coordinate mapping in quantum thermodynamics, in *Thermodynamics in the Quantum Regime: Fundamental Aspects and New Directions*, edited by F. Binder, L. A. Correa, C. Gogolin, J. Anders, and G. Adesso (Springer International Publishing, Cham, Switzerland, 2018), pp. 551–577.

[46] A. Kato and Y. Tanimura, Hierarchical equations of motion approach to quantum thermodynamics, in *Thermodynamics in the Quantum Regime: Fundamental Aspects and New Directions*, edited by F. Binder, L. A. Correa, C. Gogolin, J. Anders, and G. Adesso (Springer International Publishing, Cham, Switzerland, 2018), pp. 579–595.

[47] H. T. Quan, Y.-X. Liu, C. P. Sun, and F. Nori, Quantum thermodynamic cycles and quantum heat engines, Phys. Rev. E **76**, 031105 (2007).

[48] D. Gelbwaser-Klimovsky, W. Niedenzu, and G. Kurizki, *Thermodynamics of Quantum Systems under Dynamical Control* (Academic Press, New York, 2015), Chap. 12, pp. 329–407.

[49] K. Słowik, R. Filter, J. Straubel, F. Lederer, and C. Rockstuhl, Strong coupling of optical nanoantennas and atomic systems, Phys. Rev. B **88**, 195414 (2013).

[50] T. Hümmer, F. J. García-Vidal, L. Martín-Moreno, and D. Zueco, Weak and strong coupling regimes in plasmonic QED, Phys. Rev. B **87**, 115419 (2013).

[51] K. Le Hur, Kondo resonance of a microwave photon, Phys. Rev. B **85**, 140506(R) (2012).

[52] M. Goldstein, M. H. Devoret, M. Houzet, and L. I. Glazman, Inelastic Microwave Photon Scattering off a Quantum Impurity in a Josephson-Junction Array, Phys. Rev. Lett. **110**, 017002 (2013).

[53] B. Peropadre, D. Zueco, D. Porras, and J. J. García-Ripoll, Nonequilibrium and Nonperturbative Dynamics of Ultrastrong Coupling in Open Lines, Phys. Rev. Lett. **111**, 243602 (2013).

[54] A. Nazir and D. P. S. McCutcheon, Modelling exciton–phonon interactions in optically driven quantum dots, J. Phys.: Condens. Matter **28**, 103002 (2016).

[55] Y.-J. Wei, Y. He, Y.-M. He, C.-Y. Lu, J.-W. Pan, C. Schneider, M. Kamp, S. Höfling, D. P. S. McCutcheon, and A. Nazir, Temperature-Dependent Mollow Triplet Spectra from a Single Quantum Dot: Rabi Frequency Renormalization and Sideband Linewidth Insensitivity, Phys. Rev. Lett. **113**, 097401 (2014).

[56] D. Gelbwaser-Klimovsky and A. Aspuru-Guzik, Strongly coupled quantum heat machines, J. Phys. Chem. Lett. **6**, 3477 (2015).

[57] P. Strasberg, G. Schaller, N. Lambert, and T. Brandes, Nonequilibrium thermodynamics in the strong coupling and non-Markovian regime based on a reaction coordinate mapping, New J. Phys. **18**, 073007 (2016).

[58] G. Katz and R. Kosloff, Quantum thermodynamics in strong coupling: Heat transport and refrigeration, Entropy **18**, 186 (2016).

[59] R. Gallego, A. Riera, and J. Eisert, Thermal machines beyond the weak coupling regime, New J. Phys. **16**, 125009 (2014).

[60] A. Mu, B. K. Agarwalla, G. Schaller, and D. Segal, Qubit absorption refrigerator at strong coupling, New J. Phys. **19**, 123034 (2017).

[61] S. Restrepo, J. Cerrillo, P. Strasberg, and G. Schaller, From quantum heat engines to laser cooling: Floquet theory beyond the Born-Markov approximation, New J. Phys. **20**, 053063 (2018).

[62] D. Newman, F. Mintert, and A. Nazir, Performance of a quantum heat engine at strong reservoir coupling, Phys. Rev. E **95**, 032139 (2017).

[63] D. Newman, F. Mintert, and A. Nazir, Quantum limit to nonequilibrium heat-engine performance imposed by strong system-reservoir coupling, Phys. Rev. E **101**, 052129 (2020).

[64] M. Brenes, J. J. Mendoza-Arenas, A. Purkayastha, M. T. Mitchison, S. R. Clark, and J. Goold, Tensor-Network Method to Simulate Strongly Interacting Quantum Thermal Machines, Phys. Rev. X **10**, 031040 (2020).

[65] C. McConnell and A. Nazir, Strong coupling in thermoelectric nanojunctions: A reaction coordinate framework, New J. Phys. **24**, 025002 (2022).

[66] F. Ivander, N. Anto-Sztrikacs, and D. Segal, Strong system-bath coupling effects in quantum absorption refrigerators, Phys. Rev. E **105**, 034112 (2022).

[67] M. Kaneyasu and Y. Hasegawa, Strong coupling quantum Otto cycle, arXiv:2205.09400.

[68] A. Das and V. Mukherjee, Quantum-enhanced finite-time Otto cycle, Phys. Rev. Res. **2**, 033083 (2020).

[69] X. Y. Zhang, X. L. Huang, and X. X. Yi, Quantum Otto heat engine with a non-Markovian reservoir, J. Phys. A: Math. Theor. **47**, 455002 (2014).

[70] P. Abiuso and V. Giovannetti, Non-Markov enhancement of maximum power for quantum thermal machines, Phys. Rev. A **99**, 052106 (2019).

[71] P. A. Camati, J. F. G. Santos, and R. M. Serra, Employing non-Markovian effects to improve the performance of a quantum Otto refrigerator, Phys. Rev. A **102**, 012217 (2020).

[72] G. Thomas, N. Siddharth, S. Banerjee, and S. Ghosh, Thermodynamics of non-Markovian reservoirs and heat engines, Phys. Rev. E **97**, 062108 (2018).

[73] M. Wiedmann, J. T. Stockburger, and J. Ankerhold, Non-Markovian dynamics of a quantum heat engine: Out-of-equilibrium operation and thermal coupling control, New J. Phys. **22**, 033007 (2020).

[74] Y. Shirai, K. Hashimoto, R. Tezuka, C. Uchiyama, and N. Hatano, Non-Markovian effect on quantum Otto engine: Role of system-reservoir interaction, Phys. Rev. Res. **3**, 023078 (2021).

[75] K. Ptaszyński, Non-Markovian thermal operations boosting the performance of quantum heat engines, Phys. Rev. E **106**, 014114 (2022).

[76] N. Anto-Sztrikacs and D. Segal, Capturing non-Markovian dynamics with the reaction coordinate method, Phys. Rev. A **104**, 052617 (2021).

[77] B. Reid, S. Pigeon, M. Antezza, and G. De Chiara, A self-contained quantum harmonic engine, Europhys. Lett. **120**, 60006 (2017).

[78] J. F. Santos, C. H. Vieira, and P. R. Dieguez, Negativity-mutual information conversion and coherence in two-coupled harmonic oscillators, Physica A **579**, 125937 (2021).

[79] J. P. Cherian, S. Chakraborty, and S. Ghosh, On thermalization of two-level quantum systems, Europhys. Lett. **126**, 40003 (2019).

[80] H. Callen, *Thermodynamics and an Introduction to Thermostatistics* (Wiley, New York, 1985).

[81] M. A. Nielsen and I. L. Chuang, *Quantum Computation and Quantum Information* (Cambridge University Press, Cambridge, England, 2010).

[82] J. J. Sakurai and J. Napolitano, *Modern Quantum Mechanics*, 2nd ed. (Addison-Wesley, Boston, 2014), p. 39.

[83] G. Vidal and C. M. Dawson, Universal quantum circuit for two-qubit transformations with three controlled-NOT gates, Phys. Rev. A **69**, 010301(R) (2004).

[84] B. Kraus and J. I. Cirac, Optimal creation of entanglement using a two-qubit gate, Phys. Rev. A **63**, 062309 (2001).

[85] A. Rivas, S. F. Huelga, and M. B. Plenio, Entanglement and Non-Markovianity of Quantum Evolutions, Phys. Rev. Lett. **105**, 050403 (2010).

[86] M. M. Wolf, J. Eisert, T. S. Cubitt, and J. I. Cirac, Assessing Non-Markovian Quantum Dynamics, Phys. Rev. Lett. **101**, 150402 (2008).

[87] J. Watrous, *The Theory of Quantum Information* (Cambridge University Press, Cambridge, England, 2018).